Norgbey et al. Ecological Processes (2021) 10:10
https://doi.org/10.1186/s13717-021-00280-x

Ecological Processes

RESEARCH Open Access

Seasonal dynamics of iron and phosphorus in reservoir sediments in *Eucalyptus* plantation region

Eyram Norgbey*, Yiping Li*, Ya Zhu, Amechi S. Nwankwegu, Robert Bofah-Buah and Linda Nuamah

Abstract

Background: Iron (Fe) and phosphorus (P) dynamics in sediments have direct and indirect impacts on water quality. However, the mobility of P and Fe in reservoir sediments in *Eucalyptus* plantation region remains unclear. This study examined P and Fe pollution in sediments in a *Eucalyptus* plantation region using the novel planar optode, the ZrO-Chelex DGT, and the DIFS model.

Results: Direct in situ investigations showed that the levels of labile P and Fe were smaller in the *Eucalyptus* species-dominated sediments (X2) compared to sediments without *Eucalyptus* species (X1). The mean concentration of labile P and Fe decreased by 25% and 42% from X1 to X2. The decrement was insignificant (p = 0.20) in the surface sediment concentration for labile P. The significant disparity for DGT-Fe (Fe^{2+}) (p = 0.03) observed in the surface sediments could be attributed to the *Eucalyptus* species' elevated organic matter (tannins) concentration at X2, which reacted and consumed labile Fe. For both regions, the maximum concentration of labile P and Fe occurred in November (autumn). The reductive decomposition of Fe/Mn oxides was recognized as the main driver for their high P efflux in July and November. Low concentration of labile P and Fe was observed in December (winter) due to the adsorption of Fe/Mn oxides. The concentration of labile Fe synchronizes uniformly with that of labile P in both sediments indicating the existence of a coupling relationship (r > 0.8, p < 0.01) in both regions. The positive diffusion fluxes in both regions suggested that the sediments release labile P and Fe. The fluxes of labile P and Fe in both regions were substantially higher (p < 0.05) in the summer (anoxic period) than winter (aerobic period), indicating that hypoxia and redox conditions influenced the seasonal efflux of labile P and Fe. From the DIFS model, the replenishment ability of reactive P was higher during the anoxic period (R = 0.7, k_1 = 79.4 day^{-1}, k_{-1} = 0.2 day^{-1}) than the aerobic period (R = 0.4, k_1 = 14.2 day^{-1}, k_{-1} = 0.1 day^{-1}), suggesting that oxygen inhibited the efflux of P in the sediments.

Conclusion: Our results indicated that hypoxia, *Eucalyptus* species (organic matter (tannins)), and redox conditions influenced the seasonal mobility of sediment labile P and Fe. Our findings provided an insight into the mobility of labile P and Fe in *Eucalyptus*-dominated sediments and, moreover, serves as a reference for developing future studies on *Eucalyptus*-dominated sediments.

Keywords: Water-sediment boundary, Diffusive gradient in thin films (DGT), Planar optode, Synchronous efflux, Diffusive flux, Hypoxia

* Correspondence: ramnorg@gmail.com; liyiping@hhu.edu.cn
Key Laboratory of Integrated Regulation and Resources Development on Shallow Lakes, Ministry of Education, College of Environment, Hohai University, Nanjing 210098, China

Introduction

Sediments are a heterogeneous system that plays a significant role in water quality deterioration due to the dynamics of nutrients between the sediments and the benthic water. Recent research has shown that that the ecological degradation of water bodies owing to the mobility of phosphorus (P) and iron (Fe) at the sediment-water boundary (SWB) is a global challenge that has harmed the aquatic ecosystem (Krueger et al. 2020). Shallow water bodies are prone to sediment resuspension (via wave and wind disturbances), resulting in the efflux of nutrients from the sediments to the benthic waters. This causes the water quality of shallow water systems to be easily affected by sediment pollution compared to that of deep-water systems. Currently, the Tianbao (dominated by *Eucalyptus* trees) reservoir, which is a shallow reservoir, is experiencing water quality deterioration at an alarming pace due to the presence of Fe, P, and *Eucalyptus* species, which has resulted in changes in color and taste (Norgbey et al. 2020b). In our previous study on the Tianbao reservoir, we demonstrated that the dominant *Eucalyptus* sp. plantation was the main cause of the paroxysmal black water events in early winter (Luo et al. 2020). *Eucalyptus* species is popular in many countries because of its high economic benefit and fast growth rate. Studies by Yang et al. (2019) further revealed that black water formation in this region occurs because of the complexation reaction between Fe in sediments and tannins from *Eucalyptus* sp. trees. Other studies have attributed the black water formation in this region to the production of iron sulfide (FeS) at the SWB during hypoxia (Norgbey et al. 2020b). Due to these concerns, stakeholders and researchers are developing new techniques to improve the water quality in this region to protect the aquatic ecosystem. One way of achieving this objective is by investigating the seasonal interactions and patterns of P and Fe in the *Eucalyptus*-dominated reservoir.

Fe is a well-known element that plays a significant role in the transformation and mobility of soluble P at the SWB due to its coupling relationship with P at a micro-level (Zhang et al. 2020). Zhang et al. (2020) revealed that Fe bound P is primarily responsible for the efflux of P in sediments and the correlation between P and Fe is significant. In addition, the efflux of P has a direct relationship with the Fe/P ratio where the efflux of P decreases tremendously when the ratio is greater than 30 (Jensen et al. 1992). Other factors that primarily influence the transformation of P and Fe in freshwater systems are dissolved oxygen and oxidation-reduction potential. When oxygen is high (> 2 mg/L), Fe^{2+} is oxidized to Fe^{3+} and are present in their insoluble forms. On the other hand, when oxygen is low (< 2 mg/L), microbial reduction of Fe occurs, producing soluble forms of P and Fe into the benthic water. Although this phenomenon is common in thermally stratified reservoirs where oxygen content is low in summer and relatively high in winter (Azadi et al. 2020), studies about the efflux of P and Fe in SWB in a *Eucalyptus* species-dominated reservoir is limited. Therefore, investigating the synchronous efflux of P and Fe at the SWB at a micro-scale will help throw more light on the seasonal behavior of P and Fe in a *Eucalyptus* species-dominated reservoir.

Changes in the physical, chemical, and biological state of sediments affect the dissolved oxygen (DO) content, pH, and oxidation redox potential of sediments. Maintaining this natural state of the sediment samples during sampling will help understand the cycling of P and Fe at the SWB correctly. Currently, the use of conventional techniques in the measurement of P and Fe in sediments is accompanied by many disadvantages such as the disturbance of the physical, chemical, and biological state of sediment samples. During the transportation of the samples from the field to the laboratory, the natural state of the samples is distorted. Furthermore, the process involved in measuring samples using conventional methods is slow and cumbersome. In this study, a diffusive gradient in thin films (DGT) (based on Fick's law) was used to measure the kinetics and changes in diffusion fluxes of P and Fe at the SWB. Compared to conventional sampling techniques, the DGT technique is easy to operate and has a wide range of applicability. The DGT device can easily analyze the kinetics in P and Fe at SWB without giving ambiguous results (Luo et al. 2020). Unlike conventional techniques, the DGT technique does not contaminate or disturb the sediments during testing (Wang et al. 2016). Also, the planar optode (PO) machine examined changes in DO concentration across the SWB in 2-dimensions while the DGT-induce flux in soil (DIFS) program provided information on the replenishment ability of sediments. These high resolutions and frequency measurements provide good insight into the mechanism of P and Fe mobility at the SWB in the *Eucalyptus* species-dominated reservoir.

Currently, there is extensive literature on P and Fe mobility at the SWB for many shallow lakes. However, research on seasonal interactions of P and Fe in reservoir sediments in a *Eucalyptus* plantation region is limited. Additionally, eutrophication of reservoirs in southern China is an emerging problem (Chen et al. 2019d; Norgbey et al. 2020b), and studies on phosphorus dynamics in these reservoirs are rare. From this perspective, more dedication and studies are needed in this field to tackle the issue.

In this research, the novel PO device and the ZrO-Chelex DGT were incorporated to compare the simultaneous efflux of labile P and Fe in *Eucalyptus*-

dominated sediments to sediments without *Eucalyptus* species. This millimeter-scale technique (ZrO-Chelex DGT) has been successfully used in past studies and has proved to be a reliable way to simultaneously measure P and Fe in situ without destroying the samples (Rougerie et al. 2021). From this context, we selected the Tianbao reservoir (a shallow reservoir, dominated by *Eucalyptus* trees) as our area of study. The DGT was incorporated to synchronously calculate the interaction and pattern of P and Fe at the SWB during the different seasons in a year. Also, the DIFS model was used to investigate the replenishment ability of the sediment during hypoxia and aerobic periods in a year. The information garnered from this research can provide management knowledge (designs) on how to find long-lasting solutions to the water blackening issue in this region due to the presence of P, Fe, and *Eucalyptus* species.

Materials and methods

Study area

Tianbao reservoir-China, located within the latitude 22° 52′ 15.84′′–22° 53′ 16.51′′ N and longitude 108° 13′ 31.33′–108° 14′ 9.37′′ E, experiences black water event in early winter due to the complexation reaction between iron and tannins (Luo et al. 2020). The shallow reservoir has a volume of about 13.5 million m^3 and the watershed area of 51 km^2. Tianbao reservoir has a water surface area of 733,000 m^2 and a maximum depth of 14 m (Norgbey et al. 2020b). Tianbao reservoir is thermally stratified for a greater part of the year with no stratification occurring for a short time in winter (December to February). The reservoir is located in a subtropical monsoon climatic zone. The reservoir has an annual mean temperature of 21.9 °C and annual mean precipitation of 1304 mm. The annual mean relative humidity in this region is about 78% (Luo et al. 2020). Some parts of the reservoir are surrounded mainly by *Eucalyptus* sp. plantation. There are four main seasons in this study area: spring (March–May), summer (June–August), autumn (September–November), and winter (December–February). Two sampling points (X1, depth = 14 m and X2, depth = 10 m) were chosen in the reservoir. Sediments located at X2 are dominated by the *Eucalyptus* species, whiles X1 sediments are not close to the *Eucalyptus* species (Fig. 1). The sampling stations X1 and X2 with depths of 14 m and 10 m, respectively, were not close to activities that occur in the drainage area and the water inlet. Thus, rainfall and runoff effects were insignificant on the water quality parameters at X1 and X2.

Buoy description

A buoy was stationed at the deepest point in the reservoir with a depth of about 14 m (Fig. 1). The yellow spring instrument (YSI) multi-parameter water quality monitor (YSI EX02) was strapped to the buoy to measure the water column temperature (T), dissolved oxygen (DO), conductivity (EC), and oxidation-reduction potential (ORP). These parameters were taken on-site at an interval of 0.5 m from the surface (0.2 m) to the maximum (14 m) depth (at every 3 h interval during the day). The YSI multi-parameter and the buoy were both purchased from YSI Corporation, Yellow Springs, OH, USA. In this study, the data recorded at 12 am was used for the analysis since thermal stratification is stable and intense at this time (Liu et al. 2019). Temperature and dissolved oxygen data presented in the research work covers a period of 18 months. The trend recorded in 2018 was consistent with the trend in 2019. Thus, the

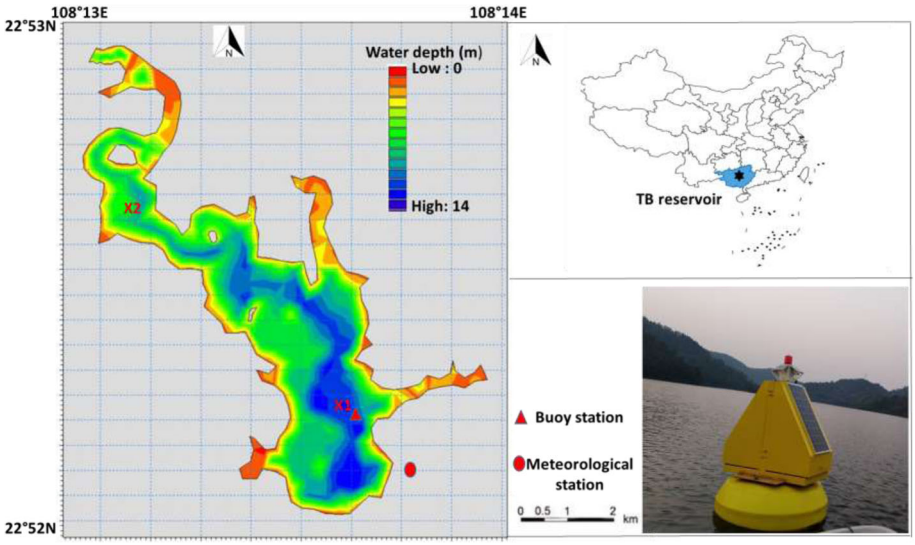

Fig. 1 Location of the study area (Tianbao reservoir)

analysis done in the study with regard to reservoir oxygen content and temperature can be depended upon to provide an unambiguous reflection of the study region.

Data collection routine

The data collection routine was done in three steps. Firstly, the water samples were collected to measure their physico-chemical properties. Secondly, the collected sediments were analyzed with DGT, PO device, and the trace metals within the sediments were measured. Thirdly, the DIFS software evaluated the resupply kinetics of P on a seasonal scale. These processes have been described in detail in the following sections.

Seasonal water quality analysis

Water samples were collected in April 2019, July 2019, November 2018, and January 2019 representing the spring season, summer season, autumn season, and winter season, respectively. Results of the received samples (water) in 2019 were consistent with water sampling done in 2018. Please see the supplementary sheet, demonstrating that the 2-year data is accurate and can be depended upon to provide an unambiguous reflection of the study region. The main reason we choose these months (April (2019), July (2019), November (2018), and January (2019)) because these periods truly reflect the peak periods of the major seasons in the study area. Specifically, April (2019), July (2019), November (2018), and January (2019) represent the peak period of spring, summer, autumn, and winter, respectively. This assertion is based on the weather temperature observed in the study area from 1960 to 2018. The weather station data has been presented in the supplementary material.

The samples (water) taken were tested for total phosphorus (TP), total nitrogen (TN), total iron (TFe), manganese (Mn), dissolved organic carbon (DOC), sulfide (S), and ammonia nitrogen (NH_3-N) at the sampling point X1 and X2 (Fig. 1). Water samples were collected using the plexiglass hydrophore water sample collector at different depths of the reservoir (0.5, 3, 6, 9, 12, 13, and 14 m). The device was obtained from the Guangxi Institute of Water Resources Research located in Nanning, China. The collected water samples were stored in a polyethylene water storage container with a volume of 500 ml. For temporary storage of the water samples, 1.0 ml of nitric acid was added to the water sample for the testing of TFe and Mn. For S, 1 ml of sodium hydroxide was added to the water sample while 1 ml of sulfuric acid was added to the water sample for the testing TP. No reagent was added to water samples for the testing of DOC. Before being sent to the research facility for further study, the water samples were held at 4 °C. Assessment of TFe and Mn was performed using the Perkin Elmer Optima 8300 ICP-OES (Inductively Coupled Plasma-Optical Emission Spectrometry), Winston-Salem, USA (Krueger et al. 2020). TP was tested in the laboratory using the ammonium molybdate spectrophotometry technique using the UV-1800 UV-Vis Spectrophotometer, Shimadzu Scientific Instrument, Columbia, USA (Shyla & Mahadevaiah 2011) while DOC was analyzed using the non-dispersive (combustion oxidation) infrared method (Bisutti et al. 2004). Sulfide in the water samples was tested following studies by Norgbey et al. (2020a, 2020b) using the methylene blue spectrophotometry. Tannins concentration in the water column was tested with the ultraviolet spectrophotometry, Shimadzu UV-1900i, Japan (Huang et al. 2018). TN was tested using the combined persulfate digestion, and NH_3-N was tested using the indophenol blue method following works done by Nwankwegu et al. (2020).

Seasonal sediment sampling

The undisturbed sediment core samples were taken from the Tianbao (*Eucalyptus* dominated) reservoir using the UWITEC sediment core sampler (obtained from Easy-Sensor Institute-Nanjing, China). The samples were collected in autumn (November 2018), winter (January 2019), spring (April 2019), and summer (July 2019). The results of the sediment samples collected in 2019 in this study were consistent with water sampling done in 2018 (See supplementary sheet), demonstrating that the 2-year data is accurate and can be depended upon to provide an unambiguous reflection of the study region. The sediment cores, with a diameter of 11 cm and length of 30 cm, were taken at X1 and X2 (Fig. 1). X1 had a depth of 14 m while X2 had a depth of 10 m. The presence of trace metals (Mn, Ni, Cu, Zn, As, Cd, Pb), total iron (TFe), total phosphorus (TP), and organic matter were measured in the surface sediments (0–25 cm). The trace metals in the surface sediments in the Tianbao reservoir were analyzed and tested using the inductively coupled plasma mass spectrometry (ICP-MS) (ThermoFisher Scientific, USA) following studies by Zhang et al. (2017). The sediment specimen was dried and passed through a plastic sieve with a size of 0.16 mm. A high-efficiency microwave digester (MLS-1200 MEG) was used to microwave the sample at a temperature of 150 °C and a digestion time of 30 min. The microwaved sieved sample was mixed with concentrated nitric acid, hydrogen peroxide, and hydrofluoric acid (ratio of 3:1:1). The samples were then tested in three replicates. The TFe in sediment samples was determined using the atomic absorption spectrophotometry (ICE 3000 Thermo Fisher Scientific – USA) while TP in the sediments was tested with the X-ray fluorescence-XRF-Rigaku Supermini200 (Fang et al. 2018). The organic matter was analyzed with the potassium dichromate-external heating method (Zhang et al. 2020).

Diffusive gradient in thin films (DGT)

DGT and PO sample analysis

The sediments at sampling sites (X1 and X2) were collected during the four seasons with the UWITEC sediment core sampler. The distribution of DO in the sediment cores was measured using the PO machine (PO2100) purchased from EasySensor Institute, Nanjing, China. Detailed information about the preparation, calibration, and usage of the PO has been provided in past research works (Yuan et al. 2020). The ZrO-Chelex DGT devices were used to simultaneously determine the variation in concentrations and the diffusive fluxes of labile P and Fe at the SWB. Before deploying the DGT device, the device (DGT) was kept in deionized water for a time of about 16 h. The deployment time for the DGT device was 24 h. After removing the DGT device from the sediment samples. The device was rinsed with deionized water, kept moist in a plastic bag and stored at a low temperature. During the deployment of the DGT devices, the PO was used to monitor the DO distribution at the SWB. To obtain information on the labile P and Fe, the ZrO-Chelex DGT was cut using the ceramic knife at an interval of 2 mm. 400 μl 1 mol/L HNO_3 was added to the binding membrane in a centrifuge tube. After 16 h of incubation, the HNO_3 was collected and tested for labile Fe. Similarly, 400 μl 1 mol/L NaOH was added to the sample and incubated for about 16 h and later tested for labile P following works by Xu et al. (2013). Detailed information about the DGT device and the simultaneous measurement of labile P and Fe have been extensively discussed and can be found in previous research works (Pedersen et al. 2015; Menezes-Blackburn et al. 2019).

DGT data analysis

The variation in concentration and the fluxes P and Fe with depth at the SWB were obtained according to Eqs. 1, 2, and 3 (Xu et al. 2013).

$$C_{\mathrm{DGT}} = \frac{M \triangle g}{DAt} \tag{1}$$

where M - amount (mass) in the device's sticking gel (ng), g - diffusive layer thickness (0.09 cm), D - coefficient of metal diffusion (cm^2/s), t - deployment time of the device (s), and A - exposure window area of the DGT device (cm^2). C_{DGT} is the concentration (effective) (mg/L)

$$\begin{aligned} F &= Fw + Fs \\ &= -D_W \left(\frac{\partial C_{DGT}}{\partial X_W}\right)_{(x=0)} \quad -\phi D_S \left(\frac{\partial C_{DGT}}{\partial X_S}\right)_{(x=0)} \end{aligned} \tag{2}$$

where F (g cm^{-2} s^{-1}) refers to the summation of benthic water and sediment fluxes, Fw (g cm^{-2} s^{-1}) refers to the labile fluxes of Fe/P from benthic water to SWB, Fs (g cm^{-2} s^{-1}) refers to the labile fluxes of Fe/P from sediment to SWB, $\left(\frac{\partial C_{DGT}}{\partial X_W}\right)_{(x=0)}$ refers to slope of concentration in the benthic water is, $\left(\frac{\partial C_{DGT}}{\partial X_S}\right)_{(x=0)}$ refers to slope of concentration in the sediment, Ds (cm^2/s) refers to the coefficients of diffusion of reactive P in the sediment, Dw (cm^2/s) refers to the coefficients of diffusion of reactive P in the benthic water, and Φ refers to the surface sediment's porosity. The porosity was measured following Eq. 3.

$$\Phi = \frac{W d_s}{(1-W)d_w + W d_s} \tag{3}$$

where W refers to mass water content, d_s refers to sediment's mean density, and d_w refers to benthic water's mean density.

DIFS model

The DIFS model, developed and first used by Harper et al. (2000), can be used to measure the remobilization of P in sediments at a micro-level. The DIFS software program parameters were obtained from Eqs. 4, 5, 6, 7, 8, 9, 10, 11.

$$Pc = \frac{W_1}{\left(\frac{W_0 - W_1}{\rho}\right)} \tag{4}$$

$$\phi_s = \frac{d_p}{(d_p + P_c)} \tag{5}$$

$$Ds = \frac{Do}{1 - \ln(\phi_s)^2} \tag{6}$$

$$R = \frac{C_{DGT}}{C_{Peeper}} \tag{7}$$

$$Kd = \frac{C_s}{C_{Peeper}} = \frac{H_1}{C_{Peeper}} = \frac{1}{P_c} \cdot \frac{k_1}{k_{-1}} \tag{8}$$

$$T_c = \frac{1}{k_1 + k_{-1}} \tag{9}$$

$$k_1 = \frac{1}{T_c} \tag{10}$$

$$k_{-1} = \frac{k_1}{k_d \cdot P_C} \tag{11}$$

where C_{DGT} refers to DGT estimated concentration (mg/L), C_s refers to solid phase concentration (mol/g), C_{peeper} refers to dissolved concentration (mg/L), R refers to DGT concentration divided by dissolved concentration, K_d refers to distribution equilibrium coefficient (cm^3/g), P_c refers to density of particle (g/cm^3), ϕ_d refers

to porosity of diffusion layer, ϕ_s refers to porosity of sediment, D_o refers to coefficients of diffusion layer (cm^2/s), D_s refers to sediment's diffusion coefficients (cm^2/s), T refers to time for deployment (h), Δg refers to thickness of diffusion layer (cm), T_c refers to time of sorption or desorption (s), k_1 refers to sorption rate constant (s^{-1}), k_{-1} refers to desorption's constant (s^{-1}), C_o refers to concentration in the gap water (mol/cm^3), H_1 refers to loosely sorbed P (mg/g), and K_d and T_c investigate the adsorption/desorption kinetics in the SWB (Harper et al. 1998, 2000).

Statistical analysis

Statistical analysis and data processing were performed. One-way ANOVA from the origin software was used to show the significant difference between different groups with a p value less than 0.05 indicating a significant difference (Huang et al. 2017). Pearson's correlation was processed using Origin software. Diagrams were drawn with Origin 9 software. Data analyses were analyzed (one-way ANOVA) using Origin 9. The sample relationship (R^2) was statistically evaluated by the linear regression analysis of SPSS Statistics 17.0 (SPSS Inc., USA). All chemical analysis determinations for sediment samples were performed in a triplicate form (Huang et al. 2019; Jiang et al. 2020; Norgbey et al. 2020a).

Results and discussion

Changes observed in the physical and chemical state of reservoir water and sediments

Variations in the physical property of reservoir water during the seasons

The seasonal changes in water column temperature (T) and dissolved oxygen (DO) content with depth at the two sampling regions (*Eucalyptus* dominated sediments and sediments without *Eucalyptus* species) have been presented in Fig. 2 and S1. The high sensor YSI machine attached to the buoy station measured the T and DO profiles at sites X1 and X2. The pH and ORP of the reservoir water over the sampling period are presented in Table S1, S2, and Fig. S1. The pH of the benthic water at X1 and X2 ranged from 6.7 to 7.2 and 6.8 to 7.3, respectively, during the seasons while the ORP ranged from 111 to 188 mV and 92 to 201 mV, respectively. The T, DO, pH, and ORP values were similar at the two sampling sites (X1 and X2) with no significant difference ($p > 0.05$).

Generally, the reservoir was thermally stratified from March to November where the water temperature decreased substantially from the surface to the bottom of the reservoir (Fig. 2 and S1). During the thermally stratified period, the mean surface (0–2 m) and bottom (11–14 m) temperatures were 28.1 °C and 15.8 °C, respectively, suggesting that the difference between the surface and bottom water temperature was significant ($p < 0.05$). The difference in surface temperature and the bottom temperature reached its lowest value in winter (December to February) where there was complete mixing of the reservoir water. In winter (no thermal stratification), the surface water temperature was 16.9 °C whiles the bottom water temperature was 15.6 °C. This trend observed in the study (2019 data) with regard to water column temperature (T) and dissolved oxygen (DO) were consistent with results measured in 2018. Please see supplementary material for the seasonal changes of water column temperature (T) and dissolved oxygen (DO) in 2018. From this context, the Tianbao reservoir can be classified as a subtropical monomictic since the reservoir experiences a single overturn period in a year (Liu et al. 2019).

The seasonal changes in the DO profiles for the reservoir (X1 and X2) are presented in Fig. 2 and S1. The entire water column in the reservoir during the mixing period (December to February) had a high DO concentration, which exceeded 6 mg/L. From March to November 2018/2019, there was a significant decline in the DO concentration of the bottom layer (11–14 m) with a value of less than 2 mg/L indicating an anoxic environment (Chen et al. 2019a). Although the bottom layer lacked oxygen during this period, the surface water layer had a high DO concentration with an average value of 8.4 mg/L. The DO concentration in the bottom water reached its lowest value (mean: 0.8 mg/L) in summer (June–August).

Variations of the chemical property of reservoir water during the seasons

From Table S1 and S2, the seasonal variation in concentrations at X1 and X2 for TP, NH_3-N, TN, S, and DOC in the water column were similar ($p > 0.05$), suggesting that the presence of *Eucalyptus* species did not influence these parameters. For both sampling regions, the concentration of TP, NH_3-N, and TN in the bottom water decrease from the anoxic period (spring, summer, and autumn) to the aerobic period (winter). The concentration of S was low (< 0.05 mg/L) in the bottom water with the difference being insignificant ($p > 0.05$) throughout the four seasons for X1 and X2. The concentration of TP (X1) in the bottom for spring, summer autumn, and winter were 0.02 mg/L, 0.03 mg/L, 0.05 mg/L, and 0.01 mgL, respectively (Table S1 and S2). The TP concentration at X1 reduced by 80% from autumn to winter. The trend was the same for X2. Similarly, the concentration of NH_3-N and TN also reduced by 55% and 52% from the anoxic season to aerobic season at X2. This indicates that the anoxic condition in the bottom water accelerated the release rate of TP, NH_3-N, and TN from the reservoir sediments to the benthic water; thus, their high concentration during the anoxic period (Nürnberg

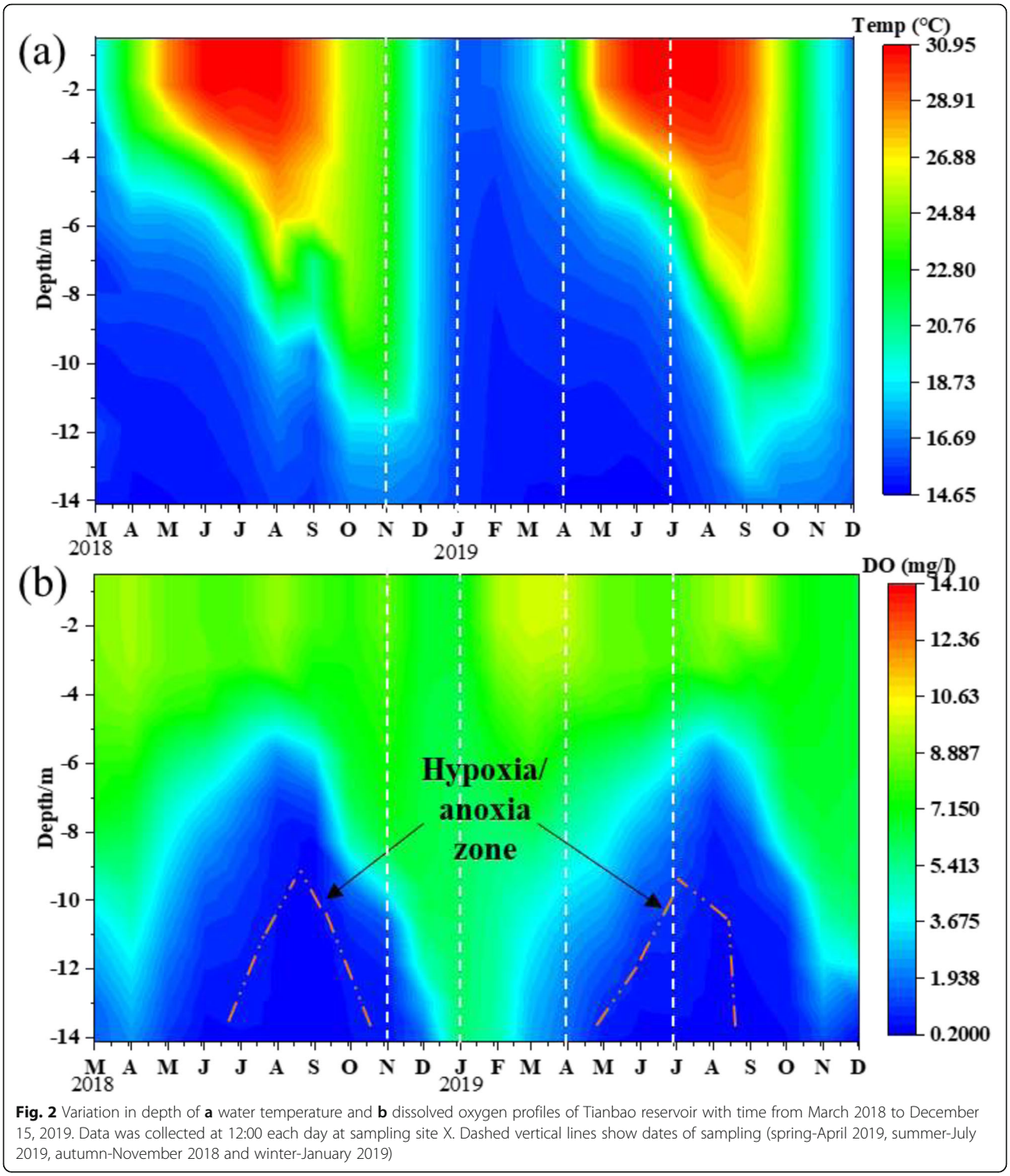

Fig. 2 Variation in depth of **a** water temperature and **b** dissolved oxygen profiles of Tianbao reservoir with time from March 2018 to December 15, 2019. Data was collected at 12:00 each day at sampling site X. Dashed vertical lines show dates of sampling (spring-April 2019, summer-July 2019, autumn-November 2018 and winter-January 2019)

2005). This trend observed in the study (2019 data) with regard to TP, NH_3-N, and TN were consistent with results measured in 2018. Please see supplementary material for the seasonal changes of TP, NH_3-N, and TN in 2018.

Variations in the physico-chemical property of sediments during the seasons

The seasonal physical (ORP and pH) and chemical properties (Mn, Ni, Cu, Zn, As, Cd, Pb, TP) in the sediments (both sampling regions) have been presented in Fig. S1,

Table S3 and S4. The difference in concentration (Mn, Ni, Cu, Zn, As, Cd, Pb, TP) between the two sampling regions were insignificant ($p > 0.05$) suggesting that the presence of *Eucalyptus* species had no primary influence on the concentration of the trace metals (Table S3). For both sampling regions, the sediment ORP showed significant ($p < 0.05$) variations across the seasons. The concentration of Mn, Ni, Cu, Zn, As, Cd, and Pb in the sediments (X1) were 769.59 mg/kg, 25.24 mg/kg, 39.26 mg/kg, 85.77 mg/kg, 13.35 mg/kg, 0.41 mg/kg, and 51.77 mg/kg, respectively, in winter. In summer, their concentration decreased by 511.88 mg/kg, 13.4 mg/kg, 22.21 mg/kg, 20.2 mg/kg, 9.82 mg/kg, 0.31 mg/kg, and 31.69 mg/kg, respectively. A similar trend was observed at sampling point X2 (Fig. S1, Table S3 and S4), with the concentration of the trace metals decreasing from winter to summer. Previous research works by (Chen et al. 2019a, 2019c) suggest that the adsorption by Fe/Mn oxides inhibits the efflux of trace metals in the sediments, thus supporting the high concentration recorded in our study in winter. From Table S3, there was a significant ($p < 0.05$) reduction in sediment's TP concentration in summer (hypoxia) compared to winter (no hypoxia) at X1 and X2. Coincidentally, the TP concentration in the bottom water was high in summer compared to that of winter (Table S1 and S2). The results suggest that significant changes in the redox conditions (Table S4) at the SWB during the different seasons influenced the concentration of trace metals and TP (Chen et al. 2019a, 2019c). This trend observed in the study (2019 data) with regard to sediment trace metals (Mn, Ni, Cu, Zn, As, Cd, Pb, TFe, TP) were consistent with results measured in 2018. Please see supplementary material for the seasonal changes of trace metals in 2018.

Studies by Jensen et al. (1992) proposed the Fe/P ratio as an indicator to describe if the sediment absorbs or releases P. This ratio helps in controlling the internal loading of P in a water system leading to eutrophication. When the Fe/P ratio is less than 15, the sediments are unable to keep soluble P (PO_4^{3-}) and release the P to the benthic water. On the other hand, when the Fe/P ratio is greater than 15, the adsorption of P occurs due to the formation of insoluble Fe/Mn oxide (in the presence of oxygen). In this study, the TFe/TP ratio at X1 during summer and winter was 13.5 and 29.3, respectively. At X2, the TFe/TP ratio was 12.3 in summer and 31.5 in winter. The low Fe/P ratio (X1 = 13.5, X2 = 12.3) for summer implied the discharge of P from the sediments to the benthic water while the high Fe/P ratio (X1 = 29.3, X2 = 31.5) in winter indicated the adsorption of soluble P by Fe/Mn oxide. The findings suggest that hypoxia caused the efflux of P from sediments in summer due to the reductive decomposition (dissolution) of Fe/Mn oxide in both the *Eucalyptus* species-dominated sediments (X2) and sediments without *Eucalyptus* species (X1) (Mortimer 1941).

Seasonal variation and coupling relationship between phosphorus and iron in the SWB

The seasonal changes of labile P and Fe^{2+} at X1 and X2 were compared (Figs. 3 and 4). For both sampling sites,

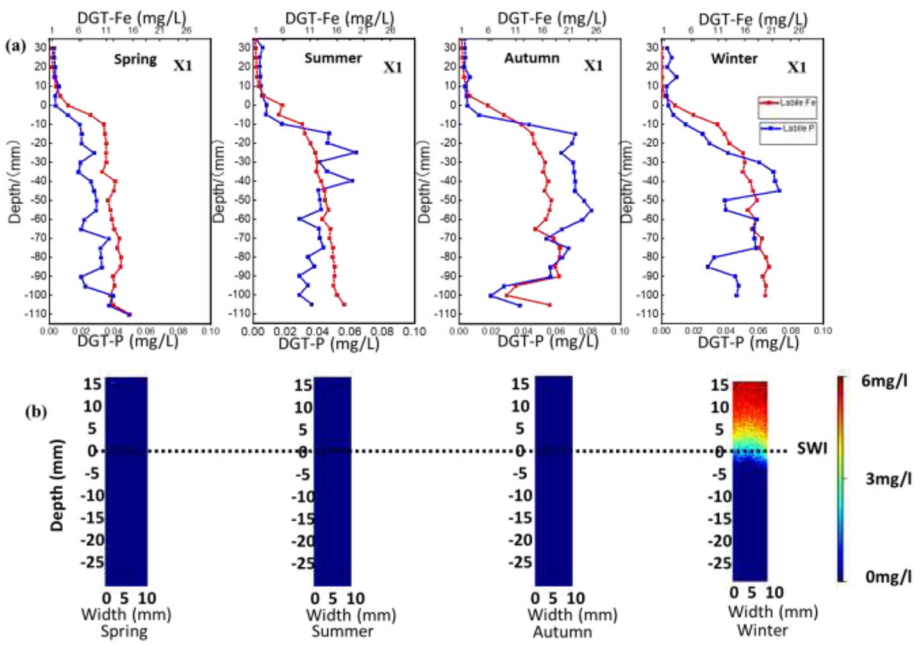

Fig. 3 Seasonal variations at sampling site X1. **a** The DGT-labile P and labile Fe concentrations with depth at the sediment-water interface (SWI) and **b** oxygen concentration at the SWI (2D imaging) of Tianbao Reservoir. The position of the SWI is represented by zero

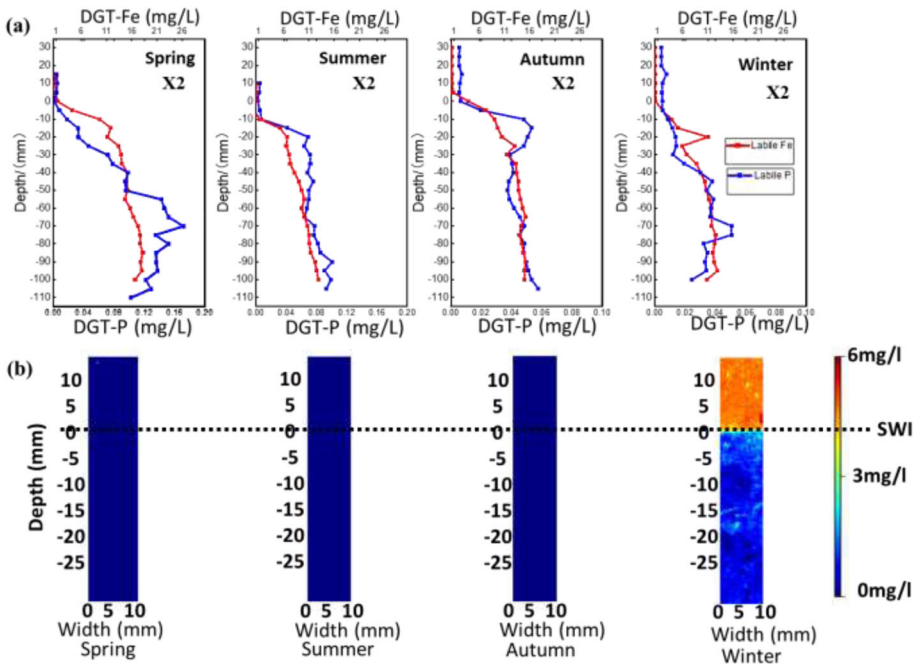

Fig. 4 Seasonal variations at sampling site X1. **a** The DGT-labile P and labile Fe concentrations with depth at the sediment-water interface (SWI) and **b** oxygen concentration at the SWI (2D imaging) of Tianbao Reservoir. The position of the SWI is represented by zero

the content of labile P and Fe showed variations suggesting that P mobility within the sediments is sensitive to redox conditions. The mean content of labile P and Fe in the surface sediment (0–30 mm) for spring (April 2019), summer (July 2019), autumn (November 2018), and winter (January 2019) in the reservoir was 9.2 mg/L, 6.7 mg/L, 11 mg/L, and 8.2 mg/L and 0.04 mg/L, 0.05 mg/L, 0.05 mg./L, and 0.02 mg/L, respectively (Table S5). For the benthic water, the mean concentration (X1 and X2) of labile Fe in spring (April 2019), summer (July 2019), autumn (November 2018), and winter (January 2019) were 0.85 mg/L, 0.93 mg/L, 1.02 mg/L, and 0.18 mg/L, respectively. While for P during this same period were 0.005 mg/L, 0.004 mg/L, 0.004 mg/L, and 0.005 mg/L, respectively (Table S5). The planar optode measured the seasonal variation in DO profiles at the SWB for X1 and X2 pictured in Figs. 3 and 4. The DO level was typically low for spring, summer, and autumn in the samples due to the intensity of thermal stratification in the reservoir. For winter, thermal stratification ceased due to the mixing of the reservoir and the DO content was significantly higher in winter compared to the other seasons (Figs. 3 and 4).

Many studies have proposed the mechanism responsible for the discharge of reactive P and Fe^{2+} from sediments to bottom water (Krueger et al. 2020). These include the reductive decomposition (dissolution) of Fe/Mn oxides by anoxia, organic matter (OM) decomposition, and changes in water environment behavior such as pH and redox potential. Other research works have shown that efflux P is sometimes dependent on Mn content (Chen et al. 2019b). For the two sampling points in this study, the sediment concentration of Mn was substantially smaller than that of Fe (Table 2). Thus, the influence of Mn on the efflux of P in the different ecotype sediments was less compared to Fe (Wang et al. 2018). In this study, the seasonal variations suggest that the hypoxia caused the Fe^{3+} ions in the sediments to be reduced to soluble Fe^{2+} ions causing the efflux of labile P within the sediment (Zhang et al. 2020), thus high labile P content from the time of hypoxia to the time of aeration. Specifically, the mean content of labile P (0–30 cm) at X1 and X2 were 0.05 and 0.04 mg/L in summer and 0.03 and 0.01 in winter, respectively. The content of labile P and Fe (for both sampling sites) was significantly smaller in the benthic water than in the sediments. The lack of oxygen within the sediments intensified the decomposition of Fe oxide and the efflux of P at the sampling sites. Thus, displaying an elevated amount of P in sediments compared to benthic water.

For a better insight on the pattern and synchronization of labile P and labile Fe, a linear correlation analysis was done between these two parameters (Fig. S2). The relationship (correlation coefficient-r^2 value) between DGT P and Fe were significantly positive during the sampling seasons at X1 and X2 (Fig. S2). The r^2 value between DGT P

and Fe at the sampling sites (X1 and X2) in spring (April 2019), summer (July 2019), autumn (November 2018), and winter (January 2019) were 0.8, 0.7, 0.8, 0.7, and 0.7, 0.9, 0.8, and 0.8, respectively. The highly significant correlation (positive) recorded ($p < 0.01$) suggested that the efflux of labile P and Fe at the SWB was synchronous and a coupling relationship existed. The gradient of the linear (correlation) equation (Fig. 4) describes the mechanism for the mobility of Fe^{2+} and reactive P at the SWB. The gradient of labile P and Fe was lower in the anoxic period compared to the aerobic period. The slopes (X1) in summer and autumn were 251.97 and 208.46, respectively, compared to 264.95 in winter. The high gradient recorded in winter revealed that sediments have a high tendency to fix P due to the presence of oxygen. Similarly, the low gradient recorded during the anoxic period shows that the sediments tend to release reactive P from the sediments (Zhang et al. 2020). A research work by Norgbey et al. (2020b) revealed that under hypoxia (reductive conditions), the complexes of Fe^{3+} are reduced to Fe^{2+}. During this process, Fe bound P decomposes and releases reactive P from the sediments to bottom water. Similarly, during the aerobic condition, Fe^{2+} is oxidized to Fe^{3+} causing the adsorption of P by Fe/Mn oxide in the sediments. The trend was similar at X2. The study showed that hypoxia enhances the efflux of labile P and Fe at both X1 and X2. The elevated concentration of labile P and Fe in summer compared to winter in both sampling sites is thus explained. Similar studies (Wang et al. 2016) were conducted in the Hongfeng reservoir (thermally stratified reservoir) in southern China where the labile P and Fe concentrations were high in summer compared to winter indicating that hypoxia influenced the process. Also, Rong et al. (2020) used the DGT (ZrO-Chelex) to measure the dynamics of P and Fe at the SWB. These authors revealed the efflux of Fe^{2+} and P was synchronous and significantly correlated, supporting the results from our study.

Role of *Eucalyptus* species in the seasonal dynamics of labile phosphorus and iron in the SWB

The seasonal (spring, summer, autumn, and winter) disparity of labile P and Fe assessed by DGT at X1 and X2 are shown in Figs. 3 and 4. The surface sediment (0–30 mm) content of labile P and Fe was lower in the *Eucalyptus* species-dominated sediments (X2) compared to sediments without *Eucalyptus* species (X1) (Table S5). The mean concentration of labile P at X1 and X2 were 0.04 ± 0.01 mg/L and 0.03 ± 0.01 mg/L, respectively. We observed an insignificant disparity (P: $p = 0.20$) in the concentration of labile P at X2 compared to X1. Similarly, the mean concentration of labile Fe at X1 and X2 were 11.1 ± 1.65 mg/L and 6.4 ± 2.8 mg/L, respectively. The significant disparity for (Fe: $p = 0.03$) DGT-Fe (Fe^{2+}) observed in the surface sediments may be attributed to the elevated content of *Eucalyptus* species at X2 (Table S4). Many research works have observed that *Eucalyptus* species have had a significant impact on soil properties. For example, the trees are known as "green deserts" because they absorb a significant amount of water in the soil (Cook et al. 2017; de Barros Ferraz et al. 2019). Yang et al. (2019) also connoted that *Eucalyptus* species affect water quality by chemically interacting with Fe to produce black products, implying that *Eucalyptus* species clearly influence the natural state of soil and water. In this study, the concentration difference of DGT-Fe at X1 and X2 (surface sediments) was statistically significant (Table S5) (Fe: p value = 0.03). Research findings (Hladyz et al. 2011; Shen et al. 2014; Li et al. 2020) have connoted that the mineralization (degradation) of organic matter process in the SWB depletes oxygen causing hypoxia (or even anoxia). Our study recorded an abundant amount of organic matter in the surface sediments of X2 compared to X1 (Table S4). In fact, the content of organic matter increased by 56% from X1 to X2. This could be attributed to the high litter-fall, root biomass in the *Eucalyptus* species-dominated sediments (X2) compared to X1. The mineralization (degradation) of organic matter process during hypoxia at the SWB facilitated the productions of Fe^{2+}/FeS from the reduction dissolution of Fe(III) oxide. This process occurs via microbial and chemical iron reduction presented in Eqs. 12 and 13, respectively (Li et al. 2020).

$$CH_2O + 8H^+ + 4FeOOH = CO_2 + 4Fe^{2^+} + 7H_2O \quad (12)$$

$$3H_2S + 2FeOOH = 2FeS + S^0 + 4H_2O \quad (13)$$

Consequently, FeS and Fe^{2+} are produced (Eqs. 12 and 13) more at X2 compared to X1 due to high organic material at X2 compared to X1. The latter interacts chemically with sulfide in the SWB (Table S3). Consequently, Fe^{2+} will dwindle at X2 compared to X1. This supports the significant reduction of DGT-Fe at X2 compared to X1.

Another reason for the dwindling of DGT-Fe at X2 compared to X1 could be the high *Eucalyptus* trees' tannins reacting with $Fe^{2+/3+}$, causing the DGT-Fe content to dwindle significantly at X2. Yang et al. (2017, 2019) deduced that the tannins from *Eucalyptus* trees are substantially greater than that of different plants. Water bodies that contain *Eucalyptus* leaves change color due to the existence of tannins (Yang et al. 2017, 2019). In this study, *Eucalyptus* trees, which are mainly concentrated at X2 compared to X1, influenced the nutrients (Fe) at the SWB. From Table S1 and S2, the mean concentration of tannins in the water column at X2 (mean 0.4 ± 0.40 mg/L) was

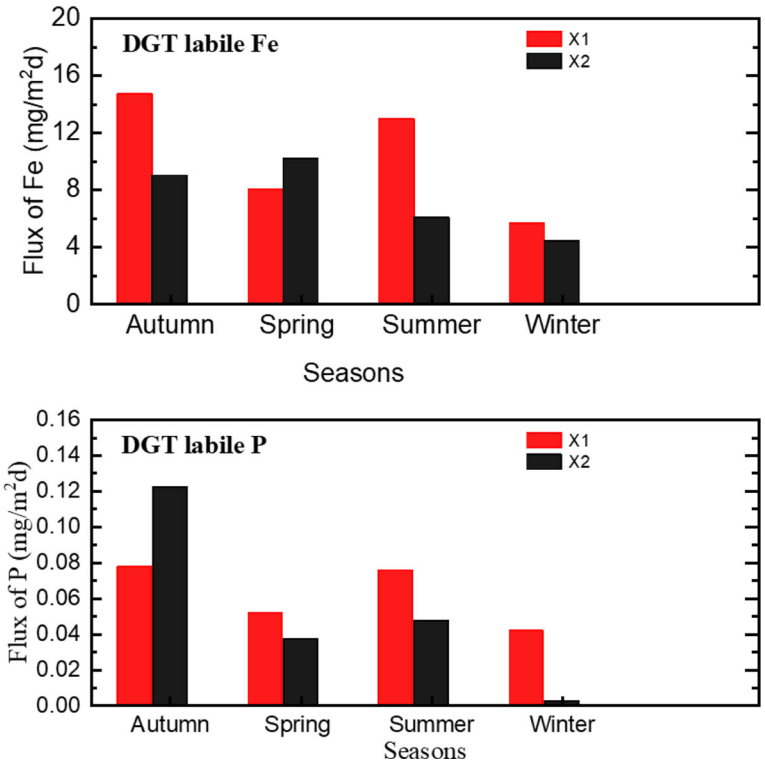

Fig. 5 The diffusive fluxes of Fe and P at the sediment-water interface in X1 of Tianbao Reservoir

higher than that of X1 (mean 0.2 ± 0.21 mg/L). In fact, the content of tannins increased by 59.5% from X1 to X2. The high *Eucalyptus* trees' tannins reacted with $Fe^{2+/3+}$, thus causing the DGT-Fe content to be used up. Yang et al. (2019) and Luo et al. (2020) have supported this assertion about *Eucalyptus* trees' tannins reacting with Fe^{2+}/Fe^{3+}. These authors further proved that *Eucalyptus* trees' tannins and $Fe^{2+/3+}$ react to produce a black substance, thus explaining the significantly low DGT-Fe concentration at surface sediment at X2 compared to X1. In short, the findings from the study showed that the *Eucalyptus* species had no significant influence on P mobility at the SWB. However, the influence of *Eucalyptus* species on the mobility of DGT-Fe was significant.

Seasonal variation in the diffusion fluxes of labile P and Fe across the SWB

The seasonal diffusive fluxes of labile P and Fe were calculated based on Fick's law (Fig. 5). The fluxes for soluble Fe^{2+} for spring, summer, autumn, and winter at X1 (X2) were 7.9 (10.1) mg m^{-2} d^{-1}, 12.9 (6) mg m^{-2} d^{-1}, 14.6 (8.9) mg m^{-2} d^{-1}, and 5.5 (4.3) mg m^{-2} d^{-1}, respectively, with no significant difference ($p > 0.05$) detected between the sediments in X1 and X2. However, a seasonal reduction (Fe^{2+}) of about 54% (28%) was observed at X1 (X2) from summer (hypoxia period) to winter (no hypoxia). Similarly, the flux for reactive P in X1 (X2) for spring, summer, autumn, and winter was 0.05 (0.04) mg m^{-2} d^{-1}, 0.08 (0.05) mg m^{-2} d^{-1}, 0.08 (0.12) mg m^{-2} d^{-1}, and 0.04 (0.002) mg m^{-2} d^{-1}, respectively ($p > 0.05$). The flux of reactive P reduced by 46% (98%) at X1 (X2) from the anoxic period to the aerobic period. The flux of reactive P at X1 (X2) was two (twenty-five) folds higher in summer than winter, suggesting that hypoxia was the primary force responsible for the efflux of reactive P from the sediments (Wang et al. 2016). During the four seasons, the diffusive fluxes of Fe^{2+} and reactive P varied and were positive (X1 and X2) indicating

Table 1 Pearson's correlation of Fe and P efflux with physico-chemical properties of Tianbao reservoir

	Fluxes	pH_{water}	ORP_{water}	DOC_{water}	$pH_{sediment}$	$ORP_{sediment}$	Organic matter-sediment	DO_{water}
X1	$J_{p\text{-}flux}$	0.09	-0.41	0.09	-0.79	-0.98	-0.69	-0.83
X1	$J_{Fe\text{-}flux}$	-0.17	-0.51	-0.01	-0.76	-0.98	-0.66	-0.82
X2	$J_{p\text{-}flux}$	0.38	-0.77	0.39	0.86	-0.73	-0.58	-0.72
X2	$J_{Fe\text{-}flux}$	-0.55	-0.17	-0.35	0.78	-0.17	-0.07	-0.6

Table 2 The input and output parameters of DIFS model for the surface (0–40 mm) sediment for summer and winter

Input										
Site	R	K_d (cm^3/g)	P_c (g/cm^3)	φ_d	φ_s	D_o (cm^2/s)	D_s (cm^2/s)	Δg (cm)	C_{DGT} (mg/L)	C_o (mg/L)
Winter	0.4	578	0.2	0.75	0.9	5.95×10^{-6}	5.1×10^{-6}	0.093	0.05	0.1
Summer	0.7	1005	0.4	0.75	0.8	5.95×10^{-6}	4.6×10^{-6}	0.093	0.04	0.05
Output										
		T_c (day)			k_1 (c)			k_{-1} (day^{-1})		
Winter		0.07			14.2			0.1		
Summer		0.01			79.4			0.2		

that both sediments acted as the source of Fe^{2+} and reactive P to the benthic water (Zhang et al. 2020). High fluxes were observed in the anoxic period whiles low fluxes were recorded during the period of no hypoxia. The high fluxes in summer in both ecotype sediments (X1 and X2) revealed that Fe^{3+} reduction promoted the release of Fe^{2+} and reactive P from the sediments (Rong et al. 2020). The mean flux of Fe^{2+} (8.8 mg m^{-2} d^{-1}) recorded in our study was substantially higher than that of the Hongfeng reservoir (average: 0.89 mg m^{-2} d^{-1}) and Lake Taihu (average: 0.85 mg m^{-2} d^{-1}) in China. Similarly, the average flux of soluble P (0.07 mg m^{-2} d^{-1}) was lower than that of the Hongfeng reservoir (average: 0.22 mg m^{-2} d^{-1}) and Lake Taihu (average: 0.15 mg m^{-2} d^{-1}), both experiencing serious eutrophication due to the presence of phosphorus (Chen et al. 2019d).

Studies have revealed that factors such as DO, pH, ORP, and organic matter strongly influence the efflux of Fe^{2+} and reactive P moving from the sediments to the bottom water (Zhang et al. 2020). Research work by Wang et al. (2016) demonstrated that sediment pH and DO content were the primary drivers responsible for the seasonal release of soluble Fe^{2+} and P in the Hongfeng reservoir, China. Similar research by Rong et al. (2020) suggested that organic matter mineralization and redox conditions contribute substantially to the high labile P fluxes in sediments. To confirm the main factors responsible for the efflux of labile P and Fe in both *Eucalyptus* species sediments and sediments without *Eucalyptus* species, the Pearson's correlation was used to explore the correlation (relationship) between the flux of labile Fe/P with their physico-chemical parameters within the sediments. The study showed that the release flux of labile P and Fe showed a strong correlation with $pH_{sediment}$, $ORP_{sediment}$, organic $matter_{sediment}$, and DO_{water} (Table 1) during the seasons in the different ecotype sediments, while the release flux of labile P and Fe showed no significant correlation with pH_{water}, ORP_{water}, and DOC_{water}. The results suggest the changes in the DO content (hypoxia/no hypoxia) at the bottom water influenced the efflux of reactive P. The results further indicated that the redox conditions, pH, and the presence of organic matter in the sediments influenced the seasonal changes in the efflux of labile P and Fe at X1 and X2.

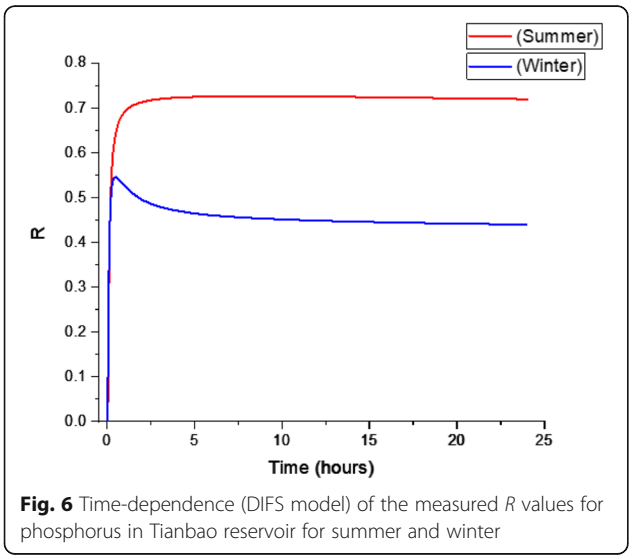

Fig. 6 Time-dependence (DIFS model) of the measured R values for phosphorus in Tianbao reservoir for summer and winter

Resupply kinetics (replenishment) of P using the DIFS model

In this study, the replenishment characteristics of P in sediments was done at X2 (*Eucalyptus* dominated sediments). The output results of the DIFS software program are pictured in Table 2. Figure 6 shows the resupply kinetics of P in the surface sediments (0–40 mm) for summer (anoxic period) and winter (aerobic period) which was simulated by the DIFS model. From Fig. 6, the resupply kinetics of P in sediments in summer can be attributed to the steady condition of "partial case" while the resupply kinetics of P in sediments in winter can be termed as the non-steady condition of "partial case" (Harper et al. 2000).

The R value provided a good analysis about the supplemental ability of reactive P (Harper et al. 1998). The mean R value for the surface sediments was higher in summer (0.7) than in winter (0.4) suggesting that the resupply ability of soluble P of the sediments is very high during hypoxia. Consequently, the T_c value during the

anoxic period was lower (0.01 day) than that of the aerobic period (0.07 day) indicating that the equilibrium time of the sediment system during the anoxic period was shorter. This means that the response time of the sediment to depletion (release reactive P) is shorter in summer compared to winter (Harper et al. 2000; Yan et al. 2019). Oppositely, the k_1 and k_{-1} values were shorter during the aerobic period (14.2 day^{-1} for k_1, 0.101 day^{-1} for k_{-1}) than the anoxic period (79.4 day^{-1} for k_1, 0.2 day^{-1} for k_{-1}) (Table 2). This revealed that a relatively high adsorption and desorption process occurred in anoxic sediment compared to the aerobic sediment (Harper et al. 2000). These results reveal that the sediment particles during hypoxia (summer) had a higher replenishment ability of phosphorus than during the aerobic period. Moreover, the findings show that the presence of oxygen in winter caused the adsorption process of Fe/Mn oxide to take place. This inhibited the efflux of P from the sediments.

Conclusion

The study investigated the seasonal dynamics of iron and phosphorus in the reservoir sediments in a *Eucalyptus* plantation region. This was achieved by using the novel planar optode, ZrO-Chelex DGT, and the DIFS model.

The study showed that there was no significant ($p > 0.05$) difference in the sediment concentration and fluxes of labile P at X1 (sediments without *Eucalyptus* species) and X2 (*Eucalyptus* species-dominated sediments), suggesting that the presence of *Eucalyptus* species did not significantly influence the efflux of labile P. However, the levels of labile Fe were significantly smaller (Fe: p value = 0.03) in the surface sediment at X2 compared to X1. This could be attributed to the elevated presence of *Eucalyptus* species' organic matter (tannic acid) content at X2, which reacted and consumed labile Fe.

The concentration and the efflux of P and Fe at the SWB were synchronous at X1 and X2. This assertion was supported by the high correlations (positive) recorded in the study at both sampling sites ($r > 0.8$, $p < 0.05$). The findings further demonstrated that hypoxia influenced the seasonal efflux of labile P and Fe at the SWB through the decomposition (reduction) of Fe(III) in both *Eucalyptus* species-dominated sediments and sediments without *Eucalyptus* species. The results also suggest the changes in the DO content (hypoxia/no hypoxia) at the bottom water influenced the seasonal efflux of reactive P, providing valuable information to stakeholders/engineers on how to control Fe/P deterioration in a reservoir by controlling the oxygen content in the benthic region since DO is the driving factor influencing the efflux of P. The measured diffusion fluxes, based on Fick's law, were positive for all the seasons and at all sampling sites (X1 and X2) suggesting that the sediments discharged labile P and Fe to the benthic water. A strong correlational relationship was pictured between labile P/Fe flux and $pH_{sediment}$, $ORP_{sediment}$, organic $matter_{sediment}$, and DO_{water} for X1 and X2, suggesting these parameters influenced the seasonal efflux of P in the *Eucalyptus* dominated reservoir. This information about the parameters (pH, DO, ORP, OM) which influence the efflux of P, serves as an indicator to stakeholders and engineers, that controlling $pH_{sediment}$, $ORP_{sediment}$, organic $matter_{sediment}$, and DO_{water} can serve as counteracting measure to control Fe/P mobility in a reservoir. The DIFS model further supported the above findings and showed that the replenishment rates of reactive P in the sediments were higher during the anoxic period (no oxygen) than the aerobic period, indicating that the adsorption process by Fe/Mn oxide (in the presence of oxygen in sediments) in winter inhibited the efflux of P from sediments. Our results gathered from this study (variations in dissolved oxygen, redox conditions, pH, and organic matter in the benthic region influence P and Fe mobility) provides valuable information to stakeholders, engineers, and researchers on understanding the geochemical transformation of P and Fe in the *Eucalyptus* dominated reservoir.

Supplementary Information

The online version contains supplementary material available at https://doi.org/10.1186/s13717-021-00280-x.

Additional file 1.

Additional file 2: Figure S1. Water temperature, dissolved oxygen, pH and redox potential variations with depth in the reservoir during the four seasons. **Figure S2**. Correlation between labile Fe and labile P in the sediments of Tianbao reservoir at A: X1 and B: X2 during the four seasons. **Table S1**. The physical and chemical characteristics of the water samples in the reservoir at sampling point X1 during the four seasons (spring, summer, autumn and winter). **Table S2**. The physical and chemical characteristics of the water samples in the reservoir at sampling point X2 during the four seasons (spring, summer, autumn and winter). **Table S3**. The chemical characteristics of the sediment in the reservoir at sampling point X1 (sediments without *Eucalyptus* species) and X2 (*Eucalyptus* dominated sediments). **Table S4**. The physical characteristics of the sediment in the reservoir at sampling points (X1 and X2) during the four seasons (spring, summer, autumn and winter). **Table S5**. Seasonal variation in the mean concentration of labile Fe and P in overlying water and sediments (0–30 mm) at sampling site (X1) of Tianbao reservoir.

Abbreviations

Fe: Iron; P: Phosphorus; SWB: Sediment-water boundary; FeS: Iron sulfide; DO: Dissolved oxygen; DGT: Diffusive gradient in thin films; PO: Planar optode; DIFS: DGT-induced fluxes in soil; YSI: Yellow spring instrument; T: Temperature; EC: Conductivity; OM: Organic matter; ORP: Oxidation-reduction potential; TP: Total phosphorus; TFe: Total iron; Mn: Manganese; S: Sulfide; NH_3-N: Ammonia nitrate; TN: Total nitrogen; DOC: Dissolved organic carbon; Mn: Manganese; Ni: Nickel; Cu: Copper; Zn: Zinc; As: Arsenic; Cd: Cadmium; Pb: Lead; R: Resupply kinetics; Kd: Distribution equilibrium coefficient; T_c: Response time of (de)sorption process; k_1: Sorption rate constant; k_{-1}: Desorption rate constant

Acknowledgements
The authors are grateful to the Guangxi Institute of Water Resources Research, Nanning, China, for their assistance during the experiment.

Authors' contributions
Conceptualization: E.N. and L.Y. Data collection and analysis: E.N, Z.Y, A.S.N, R.B.B, and L.N. Writing—original draft preparation: E.N, Z.Y, and A.S.N. Writing—review and editing: R.B.B and L.N. Supervision: L.Y. Funding acquisition: L.Y. The authors have read and agreed to the published final version of the manuscript.

Funding
The research was supported by the Chinese National Science Foundation (52039003, 51779072, 51809102). Further support came from the Fundamental Research Funds for the Central Universities (B200204014).

Ethics approval and consent to participate
Not applicable.

Competing interests
The authors declare that they have no competing interests.

Received: 9 October 2020 Accepted: 5 January 2021
Published online: 22 January 2021

References

Azadi F, Ashofteh P-S, Chu X (2020) Evaluation of the effects of climate change on thermal stratification of reservoirs. Sustain Cities Soc 102531. https://doi.org/10.1016/j.scs.2020.102531

Bisutti I, Hilke I, Raessler M (2004) Determination of total organic carbon - an overview of current methods. TrAC - Trends Anal Chem 23:716–726. https://doi.org/10.1016/j.trac.2004.09.003

Chen M, Ding S, Lin J et al (2019a) Seasonal changes of lead mobility in sediments in algae- and macrophyte-dominated zones of the lake. Sci Total Environ 660:484–492. https://doi.org/10.1016/j.scitotenv.2019.01.010

Chen M, Ding S, Wu Y et al (2019b) Phosphorus mobilization in lake sediments: experimental evidence of strong control by iron and negligible influences of manganese redox reactions. Environ Pollut 246:472–481. https://doi.org/10.1016/j.envpol.2018.12.031

Chen M, Wang D, Ding S et al (2019c) Zinc pollution in zones dominated by algae and submerged macrophytes in Lake Taihu. Sci Total Environ 670:361–368. https://doi.org/10.1016/j.scitotenv.2019.03.167

Chen Q, Chen J, Wang J et al (2019d) In situ, high-resolution evidence of phosphorus release from sediments controlled by the reductive dissolution of iron-bound phosphorus in a deep reservoir, southwestern China. Sci Total Environ 666:39–45. https://doi.org/10.1016/j.scitotenv.2019.02.194

Cook RI, Vose JM, Hall K et al (2017) Comparative water use in short-rotation *Eucalyptus benthamii* and *Pinus taeda* trees in the Southern United States. For Ecol Manage 397:126–138. https://doi.org/10.1016/j.foreco.2017.04.038

de Barros Ferraz SF, Rodrigues CB, Garcia LG et al (2019) Effects of *Eucalyptus* plantations on streamflow in Brazil: moving beyond the water use debate. For Ecol Manage 453:117571. https://doi.org/10.1016/j.foreco.2019.117571

Fang L, Shan LJ, Guo MZ et al (2018) Phosphorus recovery and leaching of trace elements from incinerated sewage sludge ash (ISSA). Chemosphere 193:278–287. https://doi.org/10.1016/j.chemosphere.2017.11.023

Harper MP, Davison W, Tych W (2000) DIFS - a modelling and simulation tool for DGT induced trace metal remobilisation in sediments and soils. Environ Model Softw 15:55–66. https://doi.org/10.1016/S1364-8152(99)00027-4

Harper MP, Davison W, Zhang H, Tych W (1998) Kinetics of metal exchange between solids and solutions in sediments and soils interpreted from DGT measured fluxes. Geochim Cosmochim Acta 62:2757–2770. https://doi.org/10.1016/S0016-7037(98)00186-0

Hladyz S, Watkins SC, Whitworth KL, Baldwin DS (2011) Flows and hypoxic blackwater events in managed ephemeral river channels. J Hydrol 401:117–125. https://doi.org/10.1016/j.jhydrol.2011.02.014

Huang H, Lv Y, Sun X et al (2018) Rapid determination of tannin in Danshen and Guanxinning injections using UV spectrophotometry for quality control. J Innov Opt Health Sci 11:1850034. https://doi.org/10.1142/S1793545818500347

Huang J, Norgbey E, Li G et al (2019) Unraveling the feeding dynamics of Chinese mitten crab-based ecosystems using carbon and nitrogen stable isotope techniques. J Consum Prot Food Saf 14:251–261. https://doi.org/10.1007/s00003-019-01220-w

Huang J, Norgbey E, Nkrumah PN et al (2017) Detection of corn oil in adulterated olive and soybean oil by carbon stable isotope analysis. J Consum Prot Food Saf 12:201–208. https://doi.org/10.1007/s00003-017-1097-x

Jensen HS, Kristensen P, Jeppesen E, Skytthe A (1992) Iron:phosphorus ratio in surface sediment as an indicator of phosphate release from aerobic sediments in shallow lakes. Hydrobiologia 235–236:731–743. https://doi.org/10.1007/BF00026261

Jiang D, Chen L, Xia N et al (2020) Elevated atmospheric CO_2 impact on carbon and nitrogen transformations and microbial community in replicated wetland. Ecol Process 9:57. https://doi.org/10.1186/s13717-020-00267-0

Krueger KM, Vavrus CE, Lofton ME et al (2020) Iron and manganese fluxes across the sediment-water interface in a drinking water reservoir. Water Res 182:116003. https://doi.org/10.1016/j.watres.2020.116003

Li B, Feng M, Chen X et al (2020) Abundant sediment organic matter potentially facilitates chemical iron reduction and surface water blackness in a Chinese deep lake. Environ Pollut 116002. https://doi.org/10.1016/j.envpol.2020.116002

Liu MM, Zhang YY, Shi K et al (2019) Thermal stratification dynamics in a large and deep subtropical reservoir revealed by high-frequency buoy data. Sci Total Environ 651:614–624. https://doi.org/10.1016/j.scitotenv.2018.09.215

Luo F, Li Y, Norgbey E et al (2020) A study on the occurrence of black water in reservoirs in *Eucalyptus* plantation region. Environ Sci Pollut Res 27:34927–34940. https://doi.org/10.1007/s11356-020-09613-3

Menezes-Blackburn D, Sun J, Lehto NJ et al (2019) Simultaneous quantification of soil phosphorus labile pool and desorption kinetics using DGTs and 3D-DIFS. Environ Sci Technol 53:6718–6728. https://doi.org/10.1021/acs.est.9b00320

Mortimer CH (1941) The exchange of dissolved substances between mud and water in lakes. J Ecol 29:280–329. https://doi.org/10.2307/2256395

Norgbey E, Huang J, Hirsch V et al (2020a) Unravelling the efficient use of waste lignin as a bitumen modifier for sustainable roads. Constr Build Mater 230:116957. https://doi.org/10.1016/j.conbuildmat.2019.116957

Norgbey E, Li Y, Ya Z et al (2020b) High resolution evidence of iron-phosphorus-sulfur mobility at hypoxic sediment water interface: an insight to phosphorus remobilization using DGT-induced fluxes in sediments model. Sci Total Environ 724:138204. https://doi.org/10.1016/j.scitotenv.2020.138204

Nürnberg GK (2005) Quantified hypoxia and anoxia in lakes and reservoirs. Sci World J 4:42–54. https://doi.org/10.1100/tsw.2004.5

Nwankwegu AS, Li Y, Huang Y et al (2020) Nitrate repletion during spring bloom intensifies phytoplankton iron demand in Yangtze River tributary, China. Environ Pollut 264:114626. https://doi.org/10.1016/j.envpol.2020.114626

Pedersen LL, Smets BF, Dechesne A (2015) Measuring biogeochemical heterogeneity at the micro scale in soils and sediments. Soil Biol Biochem 90:122–138. https://doi.org/10.1016/j.soilbio.2015.08.003

Rong N, Lu W, Zhang C et al (2020) In situ high-resolution measurement of phosphorus, iron and sulfur by diffusive gradients in thin films in sediments of black-odorous rivers in the Pearl River Delta region, South China. Environ Res 189:109918. https://doi.org/10.1016/j.envres.2020.109918

Rougerie J, Martins de Barros R, Buzier R et al (2021) Diffusive gradients in thin films (DGT): a suitable tool for metals/metalloids monitoring in continental waterbodies at the large network scale. Sci Total Environ 754:142147. https://doi.org/10.1016/j.scitotenv.2020.142147

Shen Q, Zhou Q, Shang J et al (2014) Beyond hypoxia: occurrence and characteristics of black blooms due to the decomposition of the submerged plant *Potamogeton crispus* in a shallow lake. J Environ Sci 26:281–288. https://doi.org/10.1016/S1001-0742(13)60452-0

Shyla B, Mahadevaiah NG (2011) A simple spectrophotometric method for the determination of phosphate in soil, detergents, water, bone and food samples through the formation of phosphomolybdate complex followed by its reduction with thiourea. Spectrochim Acta - Part A Mol Biomol Spectrosc 78:497–502. https://doi.org/10.1016/j.saa.2010.11.017

Wang JF, Chen JG, Ding SM et al (2016) Effects of seasonal hypoxia on the release of phosphorus from sediments in deep-water ecosystem: a case study in Hongfeng Reservoir, Southwest China. Environ Pollut 219:858–865. https://doi.org/10.1016/j.envpol.2016.08.013

Wang J, Chen J, Guo J et al (2018) Combined Fe/P and Fe/S ratios as a practicable index for estimating the release potential of internal-P in freshwater sediment. Environ Sci Pollut Res 25:10740–10751. https://doi.org/10.1007/s11356-018-1373-z

Xu D, Chen Y, Ding S et al (2013) Diffusive gradients in thin films technique equipped with a mixed binding gel for simultaneous measurements of dissolved reactive phosphorus and dissolved iron. Environ Sci Technol 47: 10477–10484. https://doi.org/10.1021/es401822x

Yan W, Liu L, Wu T et al (2019) Effects of short-term aerobic conditions on phosphorus mobility in sediments. J Freshw Ecol 34:649–661. https://doi.org/10.1080/02705060.2019.1659190

Yang G, Wen M, Deng Y et al (2019) Occurrence patterns of black water and its impact on fish in cutover areas of *Eucalyptus* plantations. Sci Total Environ 693:133393. https://doi.org/10.1016/j.scitotenv.2019.07.199

Yang X, Li D, McGrouther K et al (2017) Effect of *Eucalyptus* forests on understory vegetation and soil quality. J Soils Sediments 17:2383–2389. https://doi.org/10.1007/s11368-016-1431-4

Yuan H, Tai Z, Li Q, Liu E (2020) In-situ, high-resolution evidence from water-sediment interface for significant role of iron bound phosphorus in eutrophic lake. Sci Total Environ 706:136040. https://doi.org/10.1016/j.scitotenv.2019.136040

Zhang Y, Han Y, Yang J et al (2017) Toxicities and risk assessment of heavy metals in sediments of Taihu Lake, China, based on sediment quality guidelines. J Environ Sci 62:31–38. https://doi.org/10.1016/j.jes.2017.08.002

Zhang Z, Cao R, Mamat Z et al (2020) A study of synchronous measurement of liable phosphorous and iron based on ZrO-Chelex (DGT) in the sediment of the Chaiwopu Lake, Xinjiang, Northwest China. Environ Sci Pollut Res 27: 15057–15067. https://doi.org/10.1007/s11356-020-07701-y

Publisher's Note